

Simulation analysis of UAV autonomous landing system based on TECs

Haolin Liu, Wei Liu, Jun Xiang, Zhuoran Wang

Xi'an University of Technology, Xi'an, Shaanxi 710048

Abstract: Aiming at the decoupling control problem of velocity and altitude in the process of unmanned aerial vehicles (UAV) autonomous landing under visual guidance, this paper establishes the flight control model of fixed wing UAV, and deduces the coupling relationship between airspeed and altitude in the process of UAV glide. The total energy control system (TECs) is used for decoupling control to realize the autonomous fixed-point landing of UAV. The simulation results show that the designed control law can decouple the airspeed and altitude of the UAV, so that the UAV can land at the predetermined place autonomously and accurately.

Key words: UAV; Autonomous fixed-point landing; TECs

1. introduction

Autonomous Flight of micro UAV has always been a hot topic in the field of UAV research, and how to accurately and autonomously land the UAV after completing the set task is an urgent problem to be solved, which is of great significance for the recovery and secondary use of UAV. Predecessors have conducted many related researches on this problem. Horla and others can find the best altitude reference trajectory by using classical dynamic programming technology and change calculus, so as to form an altitude control system by imitating the reference contour. However, only path optimization is considered in takeoff and landing. Huh sunsik et al. Proposed to use a monochrome hemispherical airbag with a diameter of 4m and a height of 2m as a marker to design a vision based landing system for a micro fixed wing UAV. The control strategy is to control the aircraft to enter the target area through the direct feedback of the pitch angle and roll angle detected by the forward-looking camera in the landing phase. The problem with this method is that it is difficult to detect markers when the background is complex. In addition, the aircraft may be damaged when hitting the airbag. The visual navigation recovery scheme adopted by Gui y et al. Is to install a visible light camera integrated with DSP (digital signal processing) processor on the UAV, fix a 940nm filter in front of the lens, and use four 940nm infrared lamps as the guiding light source on the running track. Firstly, the candidate targets in the image are determined by the maximum between class variance algorithm and the region growth algorithm, and then the NLog (negative Laplacian of Gaussian) operator is used to detect and track the center of the infrared lamp in the image, and the high-precision spatial position and attitude of the UAV are calculated through coordinate transformation. Barber B proposed an algorithm based on visual feedback to accurately locate the UAV at the roughly known position of the visually identifiable target. The algorithm can deal with stationary and moving targets, and can correct camera misalignment, state estimation bias, and parameter estimation bias. Finally, the scheme of airborne visual processing and stationary target is used for testing. The results show that the proposed algorithm can guide the UAV to have a frontal impact with a 2*2m target in 12 of the 15 landing tests, and in all landing tests, the UAV landed within 5m of the target center. It can be seen that for the problem of UAV landing, there are some problems such as inaccurate landing point and poor reliability. Therefore, according to the coupling relationship between airspeed and altitude in the process of UAV landing, the total energy control system (TECs) is derived to decouple the UAV, and the TECs system simulation model is built for experimental verification.

2 design requirements for UAV autonomous positioning landing system

In order to achieve the autonomous recovery target of UAV under visual guidance, the UAV recovery process diagram adopted in this paper is shown in Figure 1. Before capturing the target landing point, the UAV relies on PIXHAWK navigation, and after capturing the target landing point, it relies on visual guidance until it hits the net.

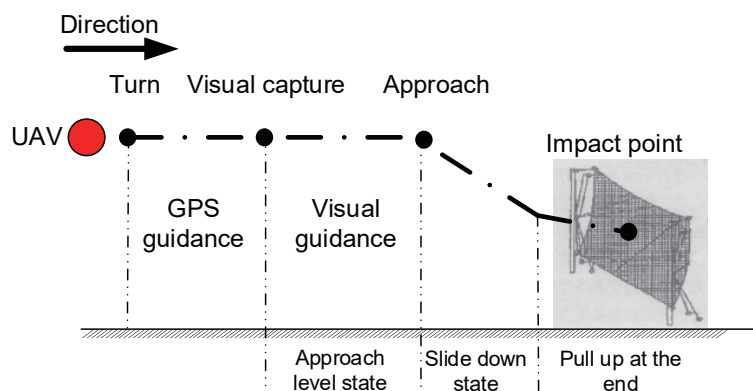


Fig. 1 Schematic diagram of UAV collision recovery

In the landing control process, there is a coupling relationship between the height and speed of the UAV in the glide guidance phase. How to carry out decoupling control is a problem that needs to be solved for the vision guided UAV.

3. establish UAV energy equation based on TECs

The total energy control system (TECs) of aircraft was proposed by Lamberts et al. In the 1980s. In order to simplify the total energy control of UAV, the following assumptions are made :

- (1) UAV is a rigid body with constant mass;
- (2) Ignoring the curvature of the ground, the ground is considered to be a plane;
- (3) It is assumed that the height does not change with time;
- (4) When the UAV is flying horizontally, it is assumed that the resistance of the UAV will not change when the state of the UAV changes.

The total energy of UAV is the sum of potential energy and kinetic energy of UAV To characterize, as shown in formula (1).

$$E_T \triangleq mgh + \frac{1}{2}mv^2 \quad (1)$$

Where, E_T Represents the total energy of UAV, g Indicates the quality of the UAV, g Represents the local gravity acceleration, h Indicates the altitude of the UAV, and v indicates the airspeed of the UAV.

The total energy change rate of UAV is the differential of formula (2) to time,

$$\dot{E}_T = mg\dot{h} + mv\dot{v} \quad (2)$$

Where, \dot{E}_T Represents the total energy change rate, \dot{h} Indicates the climb rate of UAV, \dot{v} Represents the acceleration of the UAV.

Potential energy and kinetic energy difference of UAV for total energy conversion As shown in formula (3).

$$E_D \triangleq mgh - \frac{1}{2}mv^2 \quad (3)$$

Conversion rate of total energy Is the time differential of formula (2.3), as shown in formula (4).

$$\dot{E}_D = mg\dot{h} - mv\dot{v} \quad (4)$$

The airspeed of UAV can be calculated from the perspective of energy Acceleration , height Climb rate As shown in formula (5).

$$\begin{cases} V_a = \sqrt{\left(\frac{E_T - E_D}{m}\right)} \\ \dot{V}_a = (\dot{E}_T - \dot{E}_D) \sqrt{\left(\frac{m}{E_T - E_D}\right)} \\ h = \frac{E_T + E_D}{2mg} \\ \dot{h} = \frac{\dot{E}_T + \dot{E}_D}{2mg} \end{cases} \quad (5)$$

3.1 TECs control law design

The total energy control system adopts the PI control strategy, and its control block diagram is shown in Figure 2. The role of the navigation module is to calculate the climb rate and acceleration required to reach the command altitude and airspeed according to the current altitude and airspeed of the UAV. The function of the TECs controller is to generate command thrust and command pitch angle according to the output of navigation.

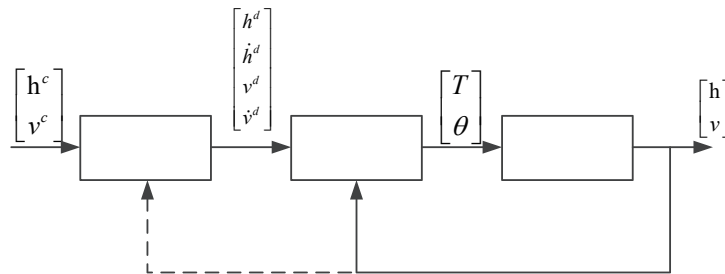


Figure 2 TECs control block diagram

Navigation module according to command height h^c And command speed Calculate the desired height h Expected climb rate \dot{h} Expected airspeed V_a Expected acceleration \dot{V}_a And calculate the desired thrust through the TECs controller T^c And desired pitch angle θ^c The UAV model reaches the specified altitude and airspeed under the action of thrust and pitch angle. The position and attitude information of the UAV is fed back to the TECs controller, and the altitude and airspeed are fed back to the navigation model. So as to form a closed-

loop airspeed and altitude controller.

Divide both sides of equations (2) and (4) by , formula (2) can be written as:

$$\dot{E}_1 = \frac{\dot{E}_T}{mgV_a} = \frac{h}{V_a} + \frac{\dot{V}_a}{g} \quad (6)$$

If track angle is assumed Very small, i.e Then formula (6) can be written as:

$$\dot{E}_1 = \frac{\dot{E}_T}{mgV_a} = \frac{h}{V_a} + \frac{\dot{V}_a}{g} = \frac{\dot{V}_a}{g} + \gamma \quad (7)$$

Formula (4) can be written as:

$$\dot{E}_2 = \frac{\dot{E}_D}{mgV_a} = \frac{h}{V_a} - \frac{\dot{V}_a}{g} = -\frac{\dot{V}_a}{g} + \gamma \quad (8)$$

Command thrust T^c and \dot{E}_1 It is a specific proportional relationship, and the command thrust is only related to the throttle size; In addition, elevator controls the conversion between unmanned maneuvering energy and potential energy, that is, the rate of energy distribution. The command thrust is calculated as shown in formula (9),

$$T^c = T_D + \Delta T \quad (9)$$

Where, T_D Represents a force that is strongly opposed to resistance, ΔT Represents thrust for energy change only, ΔT The calculation formula is shown in (10),

$$\Delta T = k_{p,T} \dot{E}_2^c + k_{i,T} \int_{t_0}^t (\dot{E}_1^c - \dot{E}_1) dt \quad (10)$$

Where $k_{p,T}$ 、 $k_{i,T}$ Represents proportional gain and integral gain respectively, \dot{E}_1^c It is the rate of change of total command energy calculated by using command acceleration and track angle. Then, the expression of command pitch angle is as shown in formula (11),

$$\theta^c = k_{p,\theta} \dot{E}_2^c + k_{i,\theta} \int_{t_0}^t (\dot{E}_2^c - \dot{E}_2) dt \quad (11)$$

Where $k_{p,\theta}$ 、 $k_{i,\theta}$ Represents proportional gain and integral gain respectively, \dot{E}_1^c Indicates the command energy allocation rate.

The proportional relationship between command acceleration and track angle is shown in formula (12).

$$\begin{cases} \dot{h}^c = k_h (h^c - h) \\ \gamma^c = \frac{\dot{h}^c}{V_a} \\ \dot{V}_a^c = k_v (V_a^c - V_a) \end{cases} \quad (12)$$

PD control is adopted in this paper for elevator adjustment generated by command pitch angle. The formula is shown in formula (13), where Indicates the pitch rate of UAV:

$$\delta_e = k_{p,\theta} (\theta^c - \theta) + k_{d,\theta} \dot{\theta} \quad (13)$$

The thrust model used in this paper is shown in formula (14),

$$T = \frac{1}{2} \rho S_{prop} C_{prop} (k_{motor}^2 \delta_i^2 - V_a^2) \quad (14)$$

Where S_{prop} Represents the area swept by the propeller, Represents air density, k_{motor} Is the aerodynamic coefficient, Is a constant determined experimentally. Formula (14) can be simplified as:

$$T = k_{T,1} \delta_i^2 - k_{T,2} V_a^2 \quad (15)$$

That is to say, the throttle control command can be calculated according to formula (16),

$$\delta_i = \sqrt{\frac{T^c + k_{T,2} V_a^2}{k_{T,1}}} \quad (16)$$

The resistance calculation formula is shown in formula (17),

$$D = \frac{1}{2} \rho S_{wing} V_a^2 C_{D0} \quad (17)$$

Where, S_{wing} Represents the wingspan and drag coefficient of UAV .

4. simulation experiment

4.1 establish UAV system simulation model based on TECs

The block diagram of the TECs control system is shown in Figure 3.

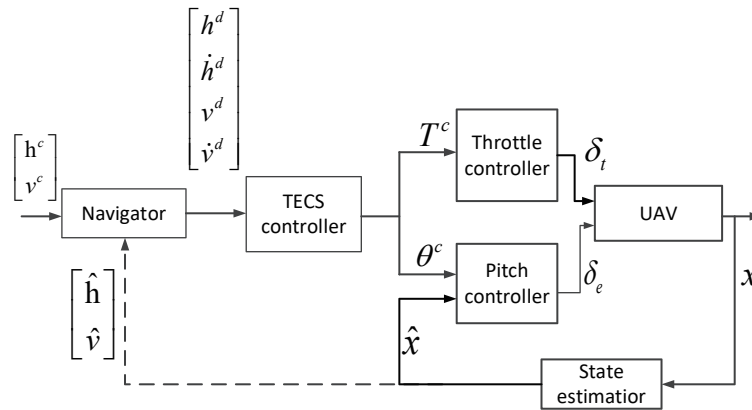


Figure 3 actual TECs block diagram

Given the command altitude and airspeed, the navigation module first calculates the acceleration and climb rate required to reach the command altitude based on the current airspeed and altitude of the UAV, and outputs the desired altitude, desired climb rate, desired airspeed and desired acceleration to the TECs controller. After obtaining the above information, the TECs controller calculates and outputs the command thrust to the throttle controller and the command pitch angle to the pitch controller. The throttle controller calculates the command throttle size through the command thrust, and the pitch controller calculates the required elevator adjustment angle through the command pitch angle and combined with the pitch angle rate of the UAV. The throttle command and elevator adjustment quantity are sent to the aircraft model, and the aircraft model makes the specified flight action to achieve the command altitude and command airspeed. At the same time, the aircraft position and attitude information is sent to the state estimation module, which sends the aircraft pitch angle rate to the pitch controller, and the altitude estimation value and airspeed estimation value to the navigation module. So as to form a closed-loop control system.

The simulation structure diagram of UAV TECs is shown in Figure 5, and the internal block diagram of TECs controller is shown in Figure 4. When the airspeed steps up and down, the UAV's altitude and throttle adjustments, as well as the airspeed and throttle adjustments in the altitude steps up and down, verify whether the TECs control method can realize the decoupling control of altitude and airspeed.

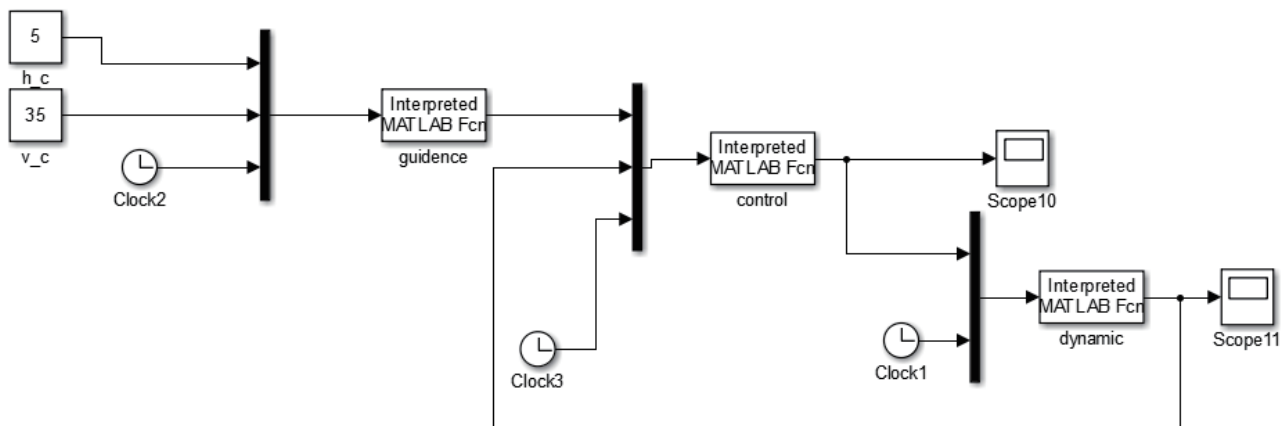


Figure 4 internal block diagram of TECs controller

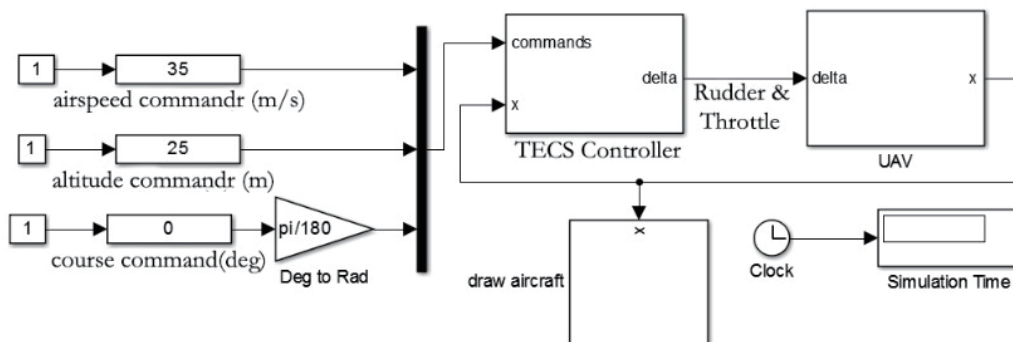


Figure 5 simulation block diagram of TECs control system

4.2 experimental results

According to the altitude and throttle adjustment of UAV during airspeed step, as well as the speed and throttle adjustment during airspeed step, to verify whether the TECs control method can realize the decoupling control of altitude and airspeed. Set parameters according to formula (12) and (13) $k_h=0.2$, $k_v=0.2$, $k_{T,1}=1.3 \times k_{T,1}$, $k_{T,1}=7.965$, $k_{T,2}=0.199$, $k_{T,2}=0$.

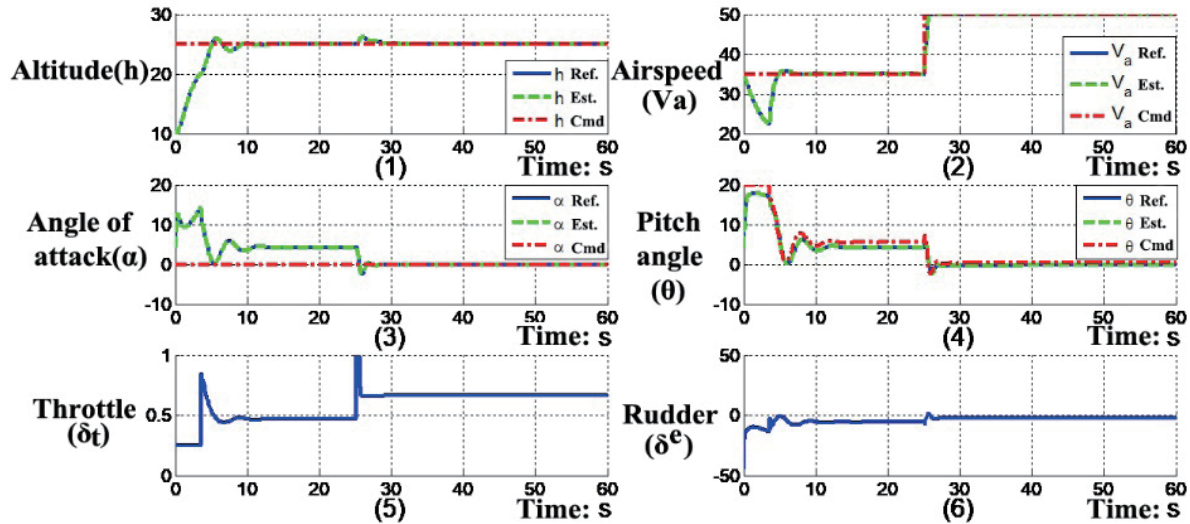


Figure 6 airspeed up step

The airspeed step simulation results are shown in Figure 6 (2). When $t=25s$, the airspeed steps from 35m/s to 50m/s, and the throttle responds quickly, as shown in Figure 6 (5). In order to increase the airspeed, the angle of attack and pitch angle drop rapidly, as shown in Figure 6 (3) and figure 6 (4). The airspeed increases, the total energy increases, and the height remains unchanged. The total energy increases through throttle adjustment, reaching a new equilibrium state. The amount of throttle at this time is significantly higher than that at the equilibrium state before the step. From the perspective of data analysis, assuming that the UAV mass is 1, the altitude does not change, and the airspeed and throttle change, in Figure 13, the airspeed changes from Jump to , total energy change The throttle changes to -0.4016.

Calculate the throttle change when the airspeed steps down $\delta t = 0.1 * \sqrt{\frac{0.2 * \frac{162.5}{30} + 0.199 * 30^2}{7.964}} \approx 0.4$ The calculated throttle changes are

consistent with the results in Figure 6 (5).

The height step simulation results are shown in Figure 14. When $t=20s$, the height steps from 35m to 20m. At this time, the airspeed suddenly decreases, the throttle decreases to 0, the elevator deflects downward, and the pitch angle decreases; After that, the airspeed is slowly adjusted to the command value, and the pitch angle and elevator are adjusted back to the command value.

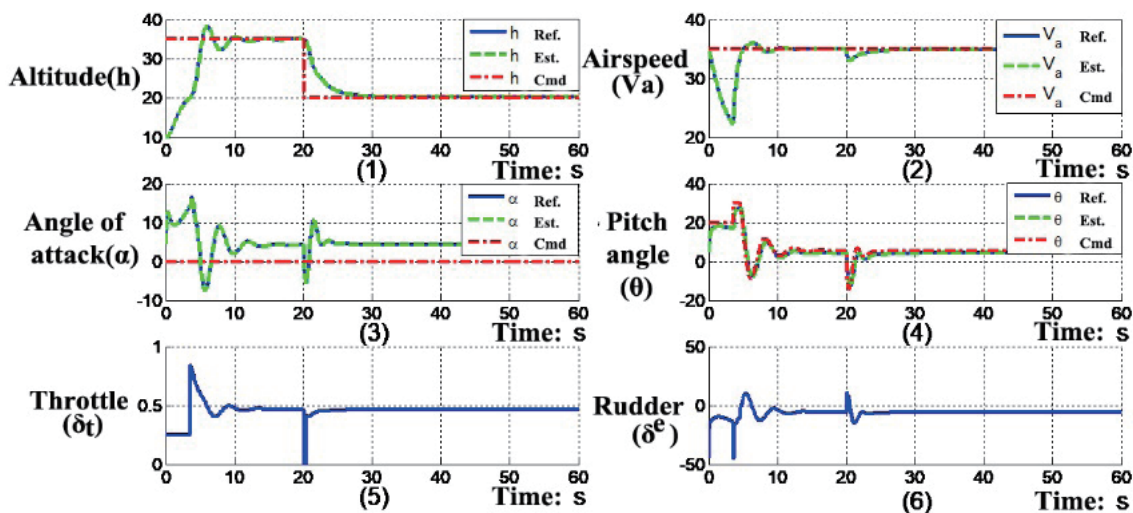


Figure 7 height down step

The simulation results show that when the airspeed step of UAV changes, the altitude of UAV remains unchanged, and the throttle adjustment is obtained through calculation. The calculation results are consistent with the simulation test results.

In conclusion, the designed TECs control law can realize the decoupling control of airspeed and altitude.

5. summary

Firstly, the decoupling control of UAV altitude and airspeed during autonomous landing is analyzed theoretically. Then, the simulation model with TECs controller is established. The TECs simulation experiment is carried out. When $t = 20s$, the simulation experiments are carried out for the step changes of airspeed and altitude respectively. The TECs control law can realize the decoupling control of airspeed and altitude, so as to realize the autonomous fixed-point landing of UAV.

References

- [1] Haolin Liu Research on vision based autonomous landing system of micro fixed wing UAV [d]Xi'an University of technology, 2018
- [2] Lea matlekovic, Filip Juric, Peter Schneider Kamp, microservices for autonomous UAV inspection with UAV Simulation as a service, simulation modeling practice and theory, volume 119, 2022
- [3] Meng y, Wang W, Han h, et al. a visual/inland integrated landing guidance method for UAV landing on the ship[j]Aerospace Science and technology, 2019, 85 (Feb.): 474-480
- [4] Horla D, cielak J On obtaining energy optimal trajectories for landing of uavs[j]Energies, 2020, 18 (8): 2062
- [5] Yapp J, seker R, babiceanu r FUAV as a service: a network simulation environment to identify performance and security issues for commercial UAVs in a coordinated, cooperative environment[c]// International Workshop on Modeling and Simulation for automotive systemstwo thousand and sixteen
- [6] Huh s, shim D h. a vision based automatic landing method for fixed wing uavs[j]Journal of Intelligent & robotic systems, 2010, 57 (1): 217
- [7] GUI y, Guo P, Zhang h, et al. airborne vision based navigation method for UAV accuracy landing using infrared lamps[j]Journal of Intelligent & robotic systems, 2013, 72 (2): 197-218
- [8] Barber B, McLain T, Edwards B. vision based landing of fixed wing miniaturization air vehicles[j]Journal of aerospace computing information & communication, 2015, 6 (3): 1-20
- [9] Kangyi Li Research on Shipborne UAV net collision recovery technology based on multi guidance system [d]Nanjing University of Aeronautics and Astronautics, 2021
- [10] Cong Zhang, Yunjie Wu, Di Fang Integrated guidance and control of fixed wing UAV automatic landing [j]Control theory and application, 2015, 32 (11): 1487-1497
- [11] Lambregts A. operational aspects of the integrated vertical flight path and speed control system[c]// Aerospace Congress and exposition1983:121-40
- [12] Zhangqingzhen Research on the application of QFT / TECs in aircraft automatic landing control [d]Northwest Polytechnic University, 2004
- [13] Bear R W, McLain t W. small unmanned aircraft: theory and practice[m]// small unmanned aircraft: theory and practice Princeton University Press, 2012
- [14] Jimenez P, Jimenez P, lichota P, et al. experimental validation of total energy control system for uavs[j]Energies, 2020, 13 (1): 14-
- [15] Banerjee a, amrr s m, Nabi MA pseudospectral method based robust optimal attitude control strategy for spacecraft[j]Advances in space research, 2019